Supplement of Atmos. Chem. Phys., 22, 14467–14488, 2022
https://doi.org/10.5194/acp-22-14467-2022-supplement

Atmospheric Chemistry and Physics
Open Access
EGU

Supplement of

Comparison of model and ground observations finds snowpack and blowing snow aerosols both contribute to Arctic tropospheric reactive bromine

William F. Swanson et al.

Correspondence to: William F. Swanson (wswanson3@alaska.edu)

1. Supplement

Supplemental Equations

$$\mathbf{A_c} = \mathbf{W^* A_f W} \quad \text{(S1)}$$

A_c is the coarse averaging kernel, A_f is the fine averaging kernel, W is the interpolation matrix which samples the coarse grid profile vector on the fine grid, and W* is the transformation matrix (Payne et al., 2009).

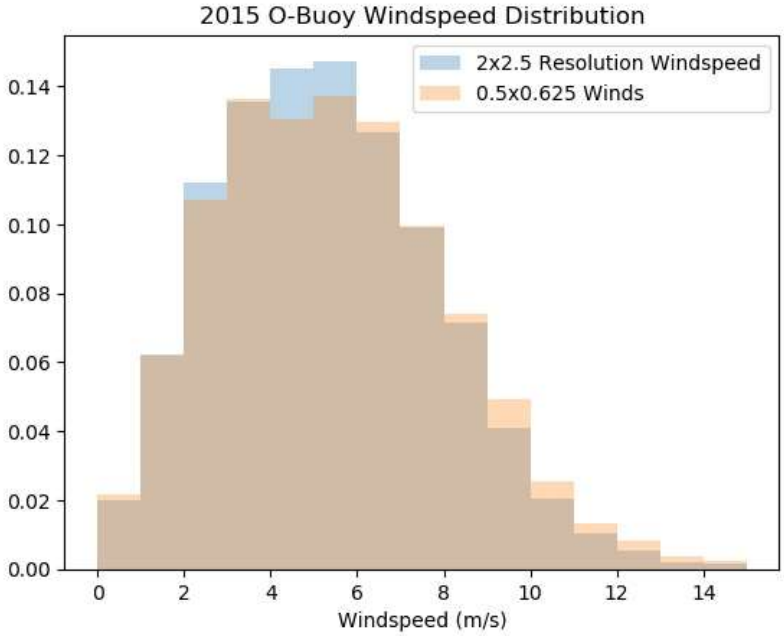

Supplemental Figure S1: Windspeed histogram

Distribution of windspeed along O-Buoy paths, plotted by bins of 1 m/s. Windspeed is in units in m/s, while Y-axis shows fraction of all windspeeds along O-Buoy paths in each bin.

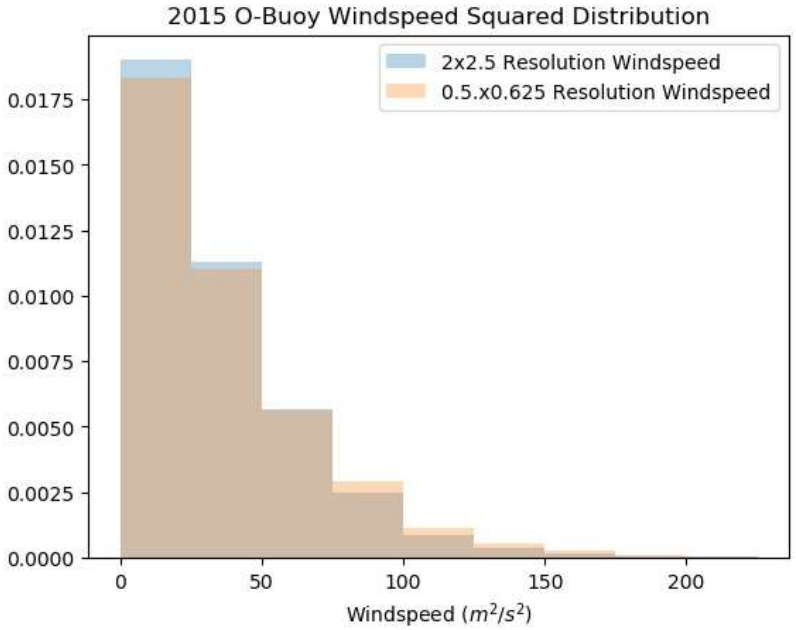

Supplemental Figure S2: Windspeed squared histogram

Distribution of windspeed squared along O-Buoy paths, plotted by bins of 25 m^2/s^2. Windspeed is in units in m/s, while Y-axis shows number of observations in each bin.

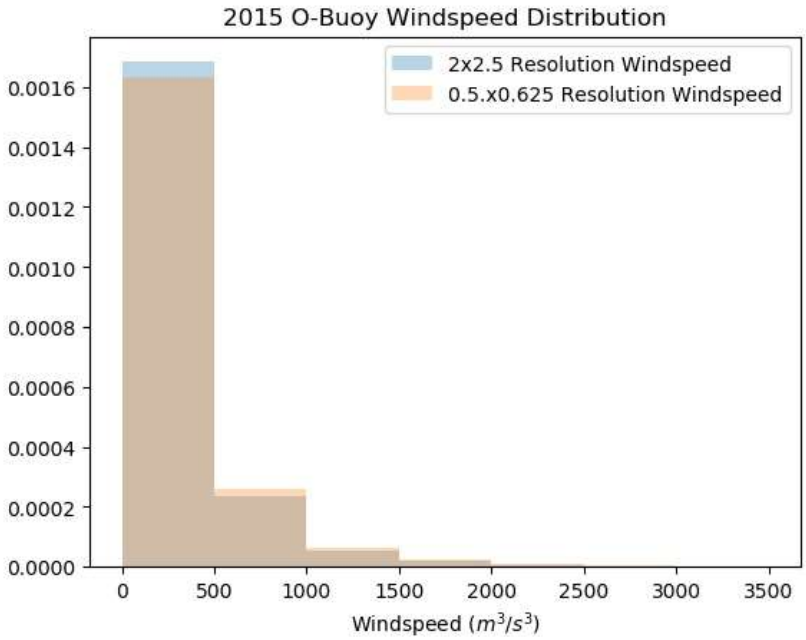

Supplemental Figure S3: Windspeed cubed histogram

Distribution of windspeed cubed along O-Buoy paths, plotted by bins of 500 m^2/s^2. Windspeed is in units in m/s, while Y-axis shows number of observations in each bin.

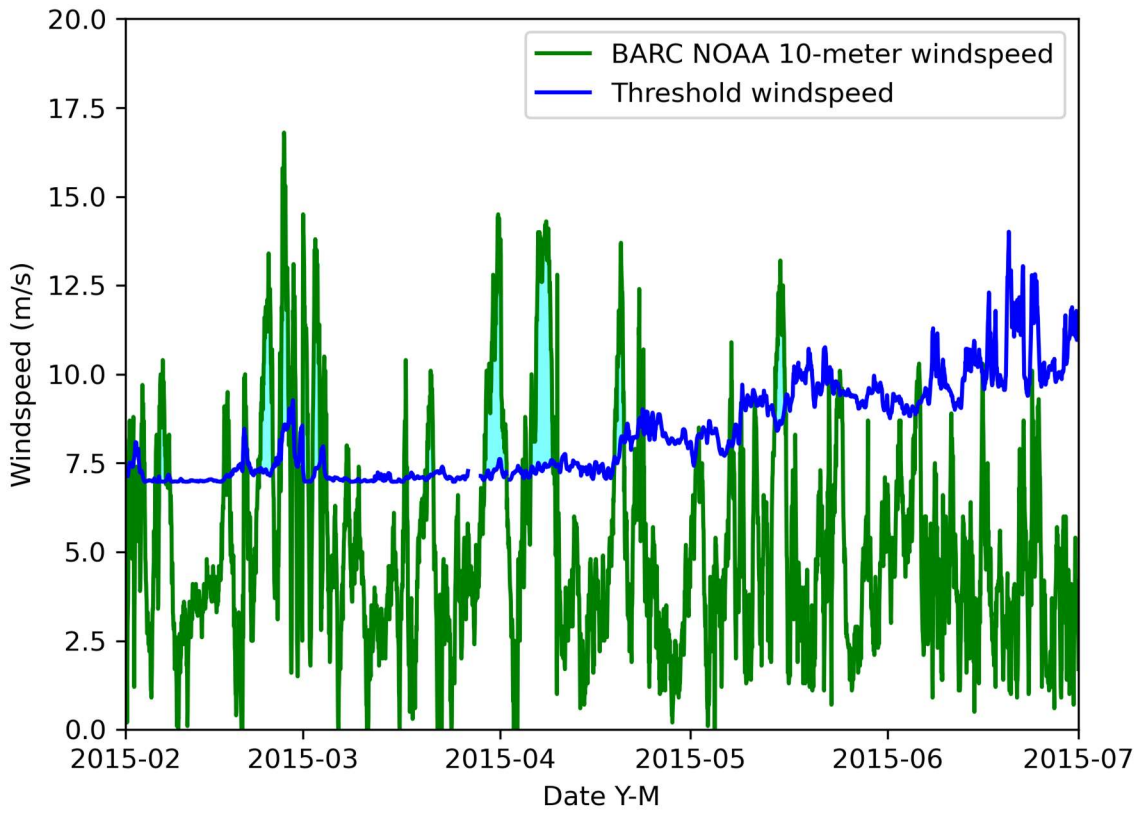

Supplemental Figure S4: Utqiaġvik ten-meter windspeeds

Hourly ten-meter windspeeds measured at Barrow Arctic Research Center (BARC) in green (NOAA, 2018), with threshold windspeed calculated from BARC ten-meter temperature using Equation 1 in blue. Periods with the potential for blowing snow SSA production highlighted in cyan.

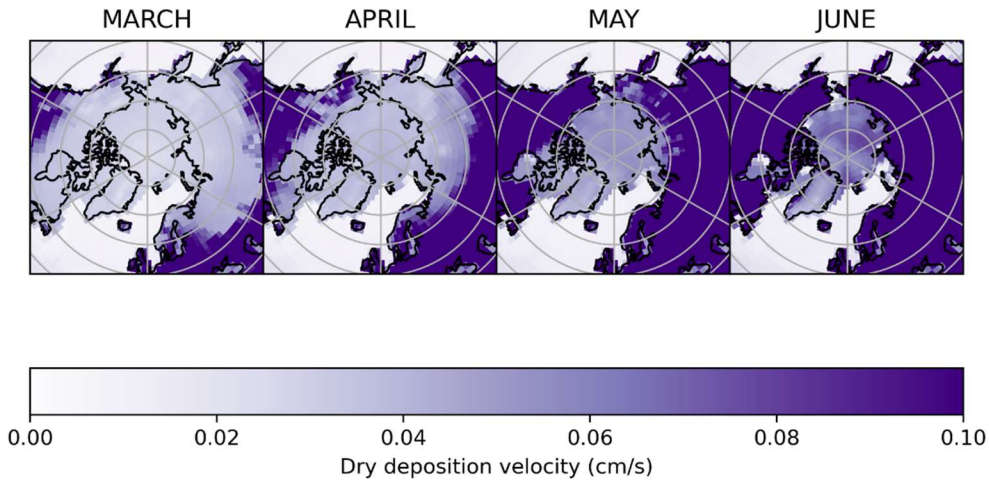

Supplemental Figure S5: Ozone dry deposition velocities by month, as simulated by GEOS-Chem

The dry deposition velocity of ozone in GEOS-Chem from 50 º N to 90 º N region in cm/s at 2° latitude x 2.5° longitude spatial resolution.

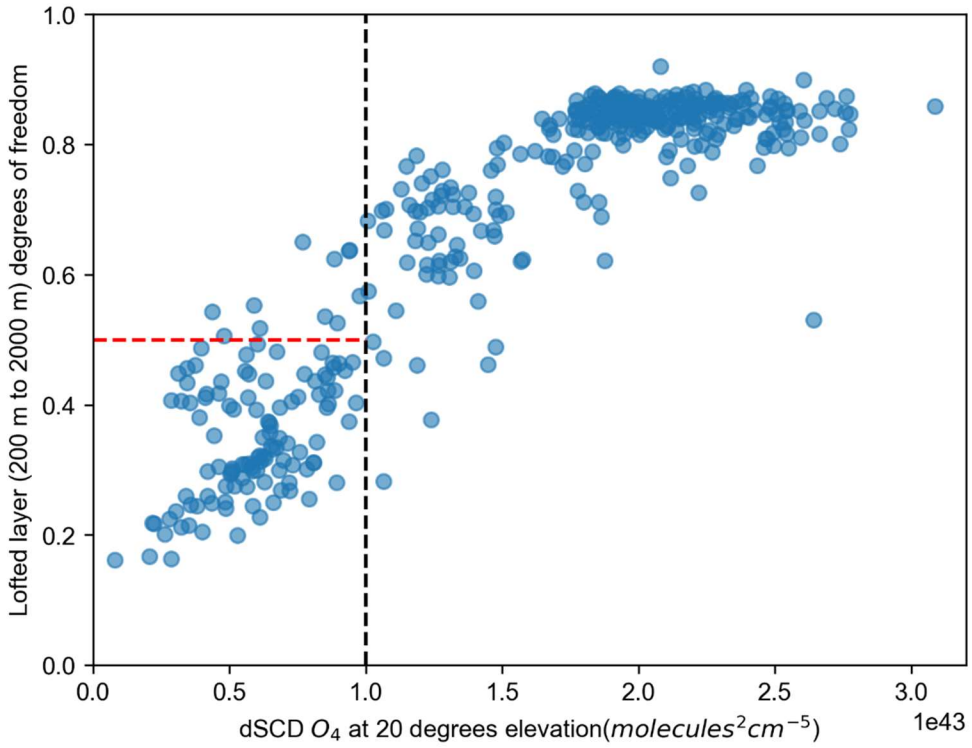

Supplemental Figure S6: Clear sky screen

Degrees of freedom in the lofted later from 200 to 2000 m plotted versus slant column density of the O_4 collisional dimer at 20º elevation. The clear sky threshold at 0.5 degrees of freedom is shown by the dashed red line, with the BrO_{LTcol} screen threshold at 10^{43} molecules^{2}cm^{-5} dSCD O_4 shown by dashed black line.

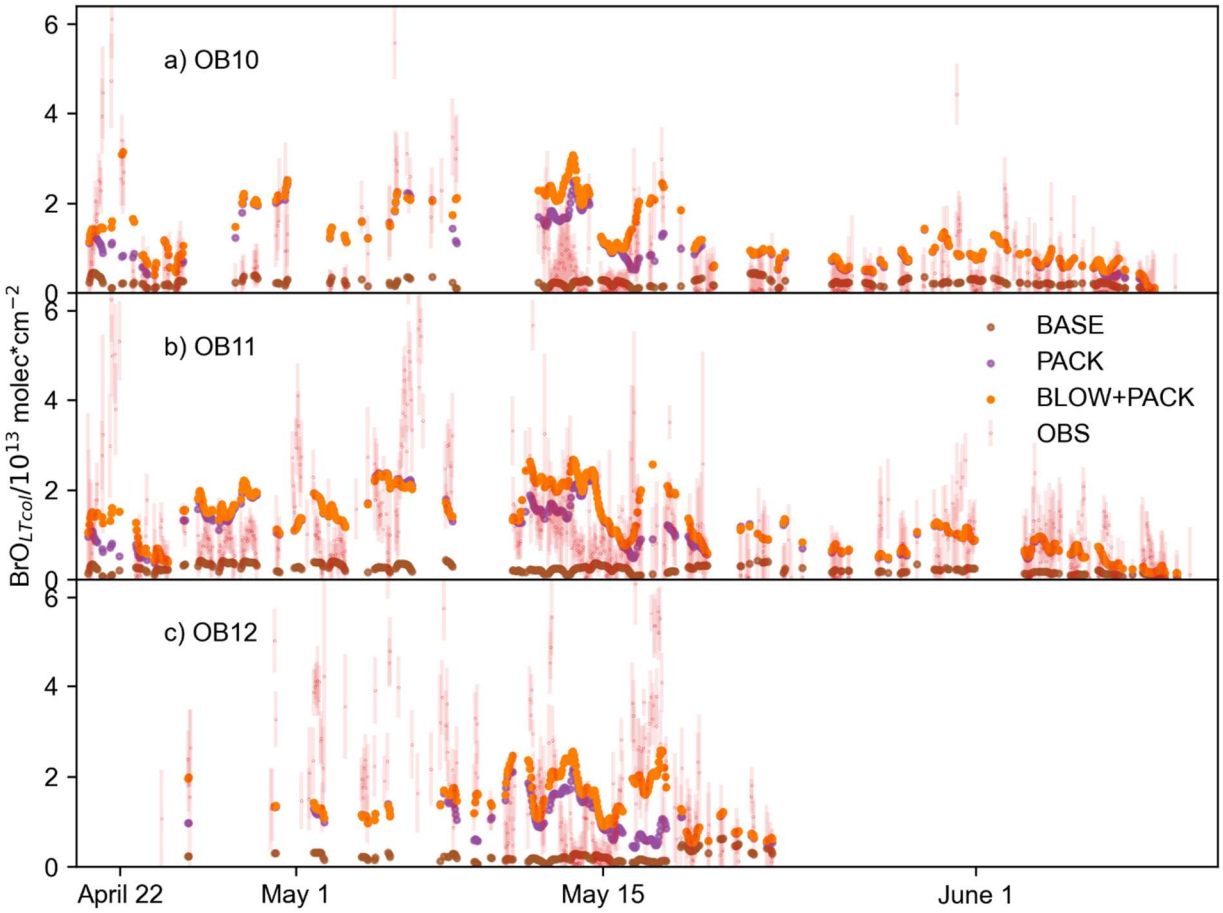

Supplemental Figure S7: Utqiaġvik Hourly BrO_{LTcol} timeseries
Hourly timeseries of BLOW+PACK, PACK, and BASE BrO_{LTcol} on a) O-Buoy 10, b) O-Buoy 11, and c) O-Buoy 12 in the 2015 Arctic Spring. O-Buoy observations and error bars in red, BASE BrO_{LTcol} in brown, PACK BrO_{LTcol} in purple, and BLOW+PACK BrO_{LTcol} in orange. All BrO_{LTcol} and model BrO_{LTcol} plotted as points where each model prediction corresponds to a valid screened BrO_{LTcol} observation.

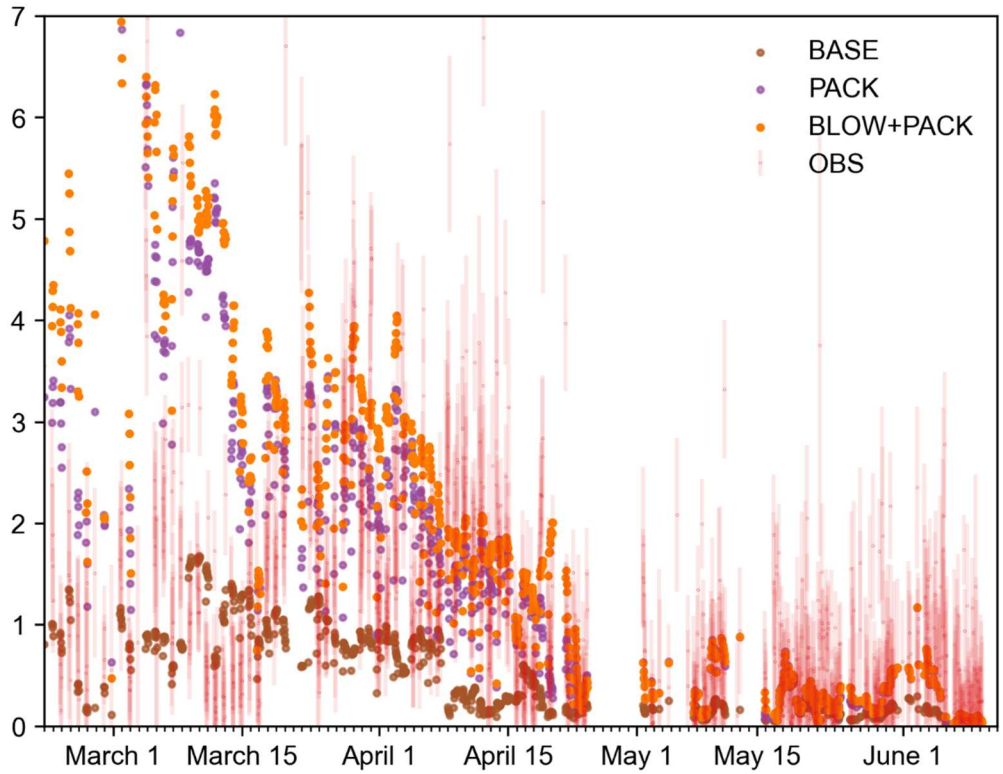

Supplemental Figure S8: Utqiaġvik Hourly BrO_{LTcol} timeseries
Hourly timeseries of BLOW+PACK, PACK, and BASE BrO_{LTcol} at BARC, Utqiaġvik in the 2015 Arctic Spring. Observations and error bars in red, BASE BrO_{LTcol} in brown, PACK BrO_{LTcol} in purple, and BLOW+PACK BrO_{LTcol} in orange. All BrO_{LTcol} and model BrO_{LTcol} plotted as points where each model prediction corresponds to a valid screened BrO_{LTcol} observation.

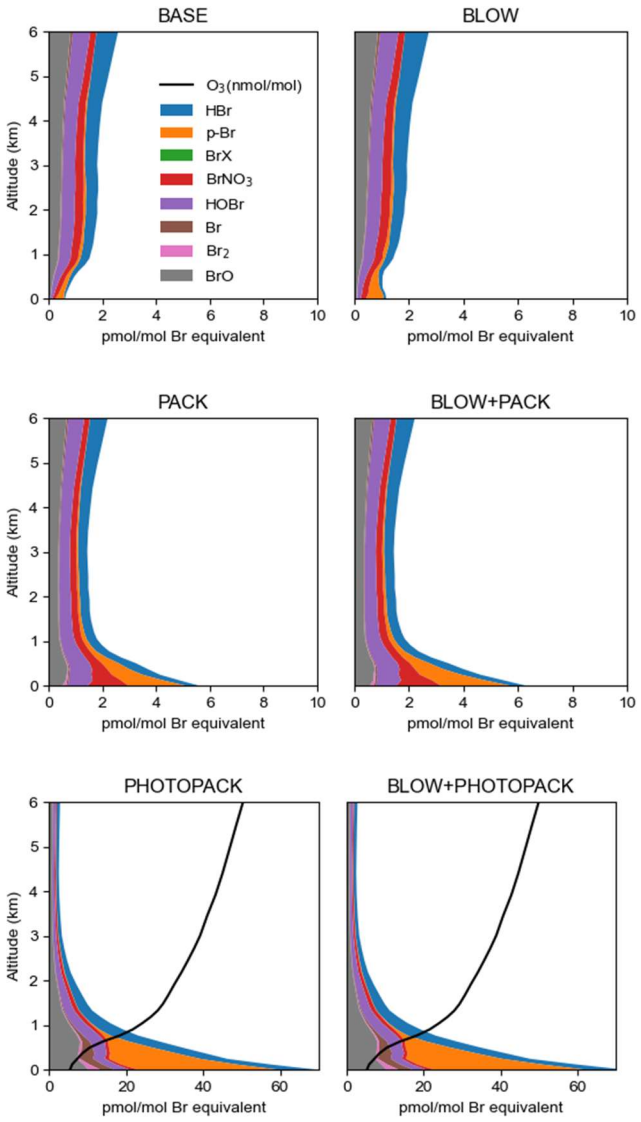

Supplemental Figure S9: Simulated vertical profiles of Br_y and p-Br^- at Utqiaġvik in May 2015.

Mixing ratios of Br equivalent (true Br_2 mixing ratios are half of plotted Br ratios) are shown for daytime (solar elevation > 5°). The simulations are named in the panel titles. Ozone is plotted in black as nmol/mol for PHOTOPACK and BLOW+PHOTOPACK runs.

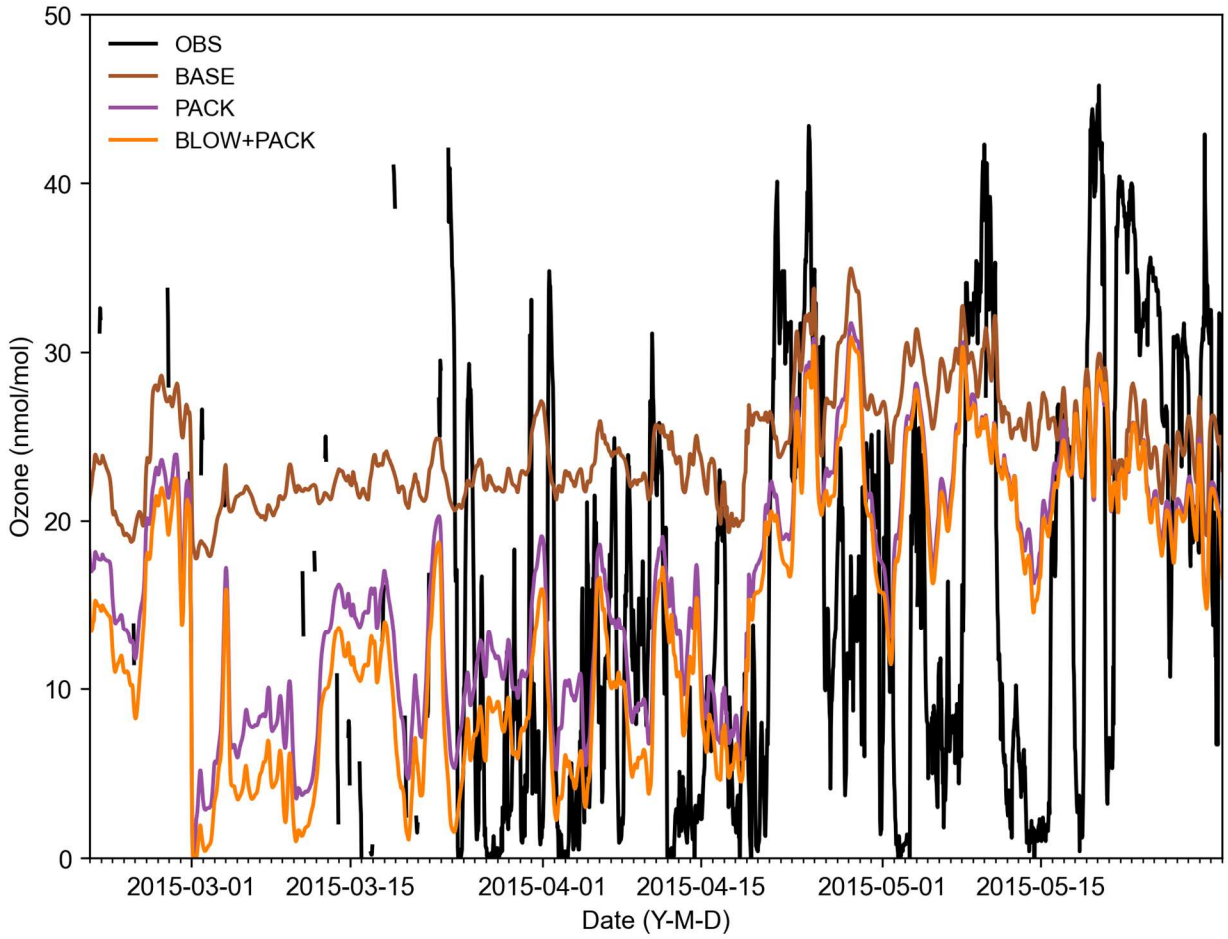

Supplemental Figure S10: Hourly O-Buoy 11 ozone timeseries
Hourly timeseries of BLOW+PACK, PACK, and BASE ozone on O-Buoy 11 in the 2015 Arctic Spring. Ozone observations from O-Buoy in black, BASE ozone in brown, PACK ozone in purple, and BLOW+PACK ozone in orange. Gaps indicate missing observational data.

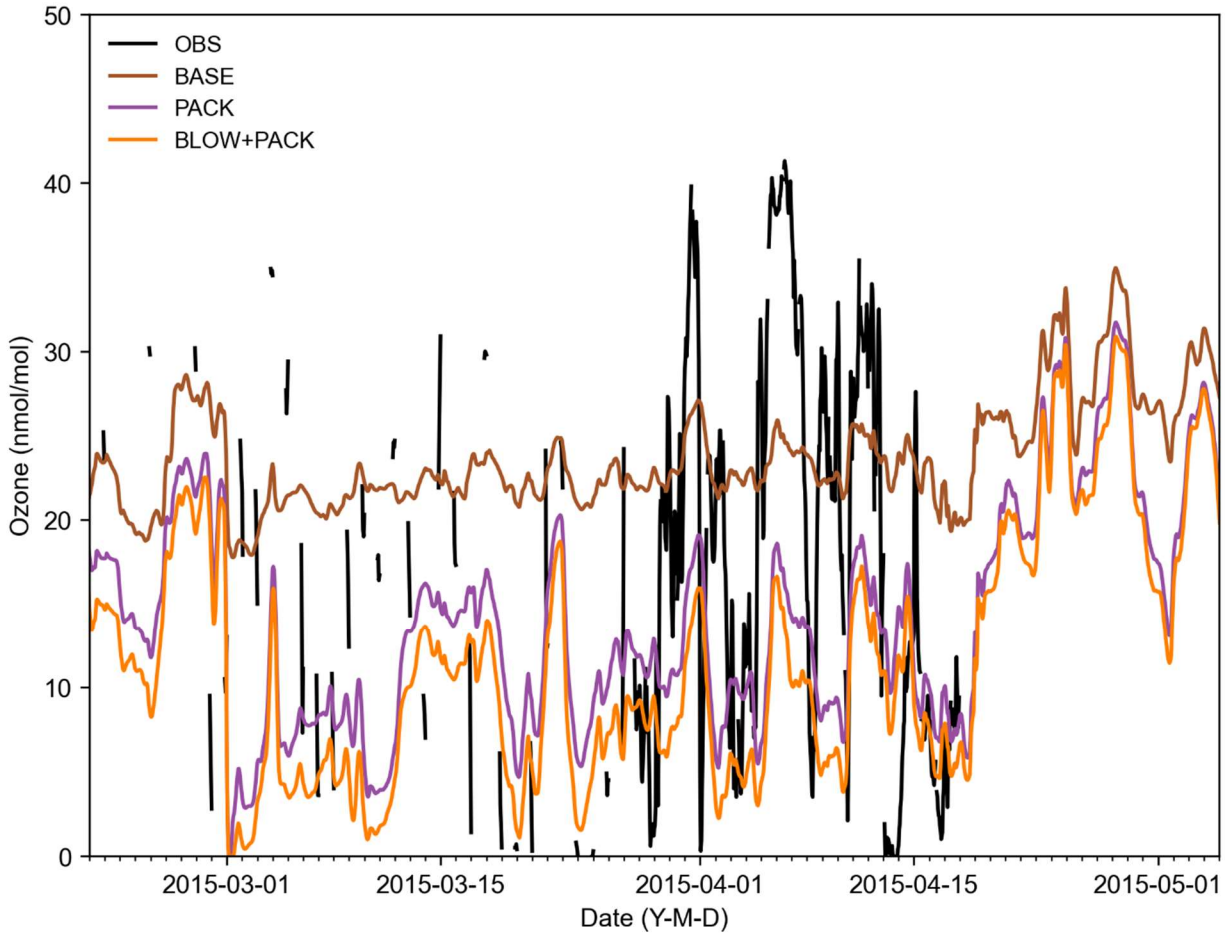

Supplemental Figure S11: Hourly O-Buoy 12 ozone timeseries
Hourly timeseries of BLOW+PACK, PACK, and BASE ozone on O-Buoy 12 in the 2015 Arctic Spring. Ozone observations from O-Buoy in black, BASE ozone in brown, PACK ozone in purple, and BLOW+PACK ozone in orange. Gaps indicate missing observational data.

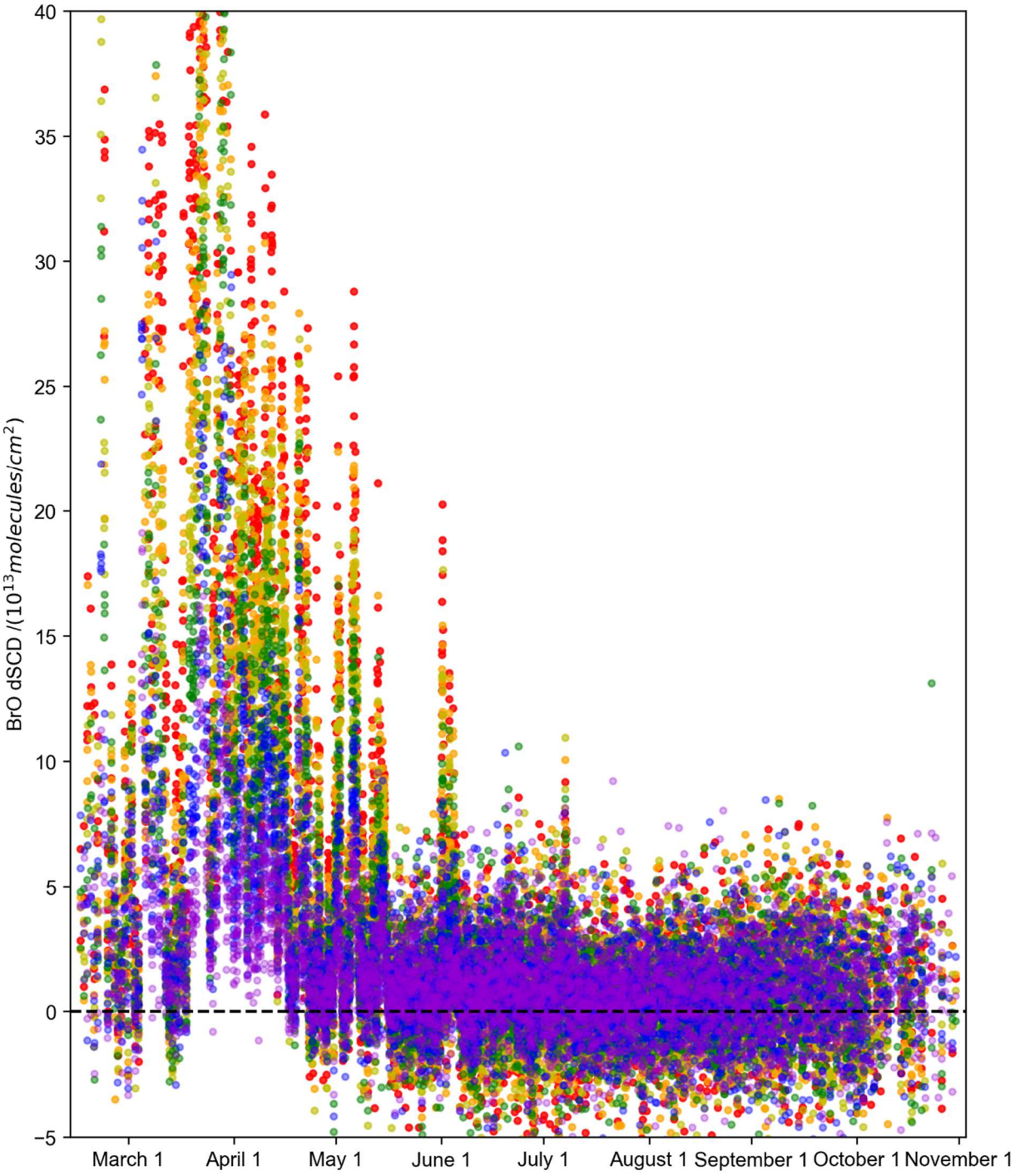

Supplemental Figure S12: Utqiaġvik 2015 differential slant column densities

Differential slant column densities of BrO at the Barrow Arctic Research Center from February through November 2015. View angle is denoted by color: 1° is red, 2° is orange, 3° is yellow, 5° is green, 10° is blue, and 20° is violet.

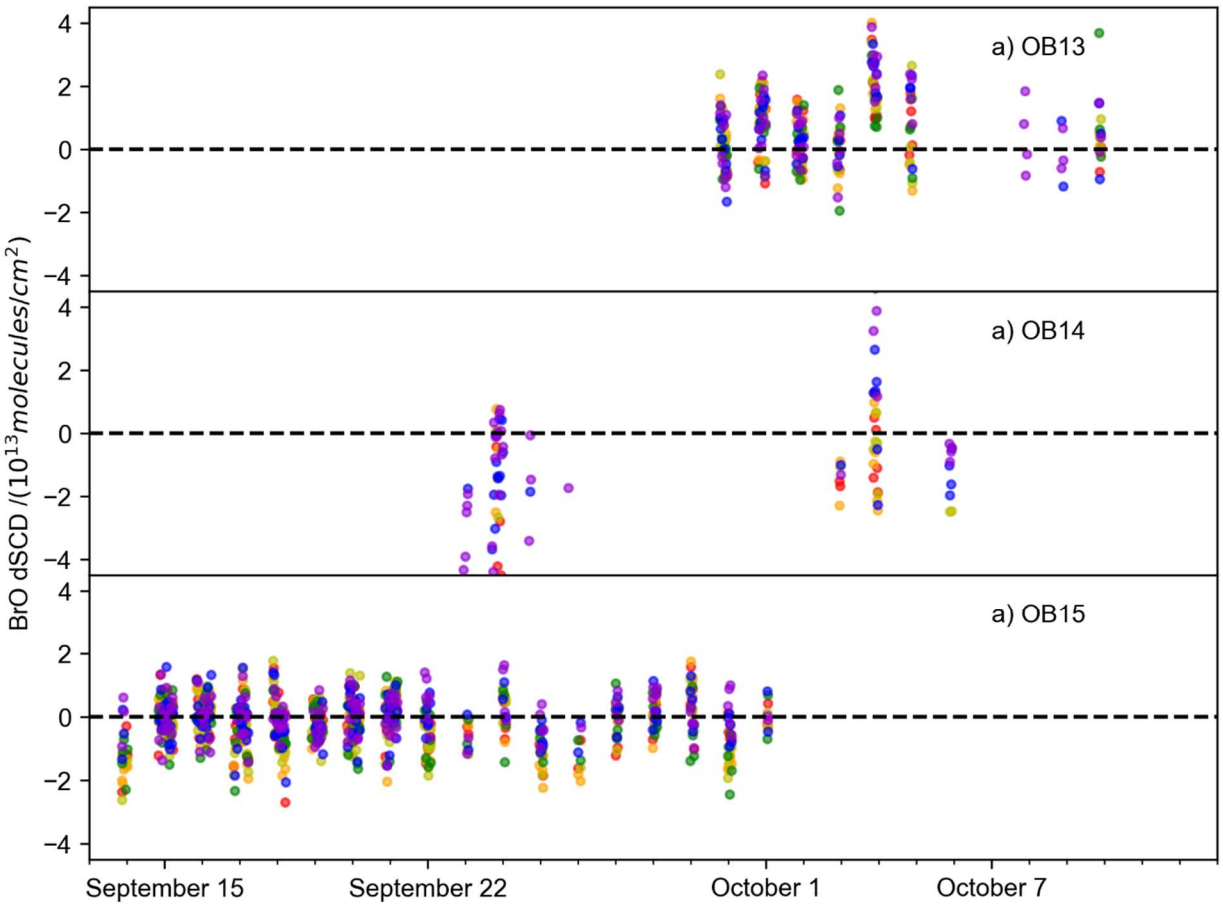

Supplemental Figure S13: O-Buoy Fall 2015 differential slant column densities

Differential slant column densities of BrO at each buoy from September 13-October 13. View angle is denoted by color: 1° is red, 2° is orange, 3° is yellow, 5° is green, 10° is blue, and 20° is violet.

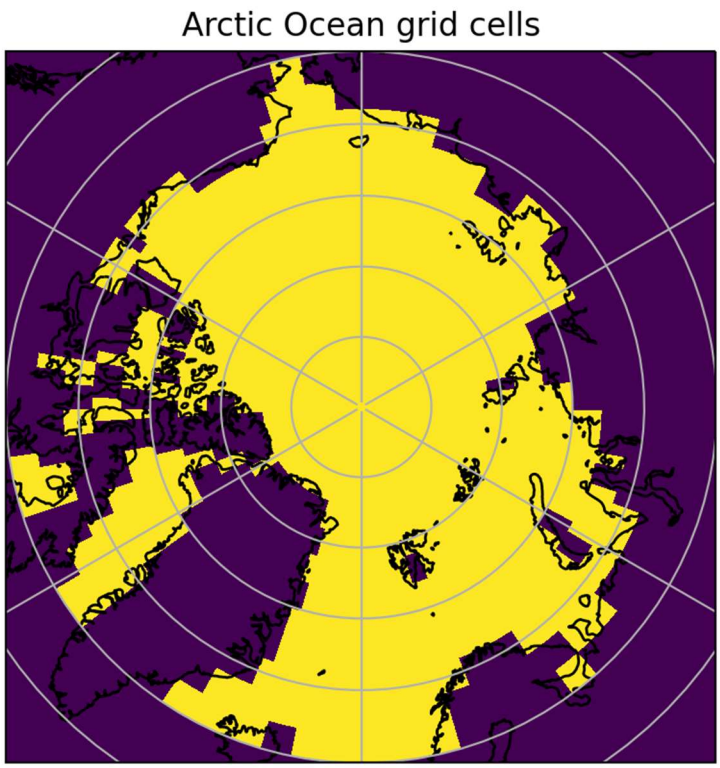

Supplemental Figure S14: Arctic Ocean grid cells in GEOS-Chem

Shows the area over which the burdens and rates in Table 2 were calculated. Yellow coloring indicates a grid cell north of 66˚ N latitude with greater than 50% fractional ocean coverage as determined by MERRA-2 ocean fields.